$BaCu_3O_4$: High-temperature magnetic order in one-dimensional $S = \frac{1}{2}$ diamond chains

C. W. Rischau,[1] B. Leridon,[1,*] D. Colson,[2] A. Forget,[2] and P. Monod[1]

[1]*Laboratoire de Physique et d'Etude des Matériaux, UMR8213 CNRS-ESPCI ParisTech-UPMC, 10 rue Vauquelin, 75231 Paris Cedex 05, France*

[2]*Service de Physique de l'Etat Condensé, Orme des Merisiers, IRAMIS, CEA-Saclay (CNRS URA 2464), 91191 Gif sur Yvette Cedex, France*

(Received 9 January 2012; published 16 April 2012)

The magnetic properties of the alkaline-earth oxocuprate $BaCu_3O_4$ are investigated. We show that the characteristic Cu_3O_4 layers of this material can be described with diamond chains of antiferromagnetically coupled Cu 1/2 spins with only a weak coupling between two adjacent chains. These Cu_3O_4 layers seem to represent a so far unique system of weakly coupled one-dimensional magnetic objects where the local antiferromagnetic ordering of the Cu^{2+} ions leads to an actual net magnetic moment of an isolated diamond chain. We demonstrate a magnetic transition at a high Néel temperature $T_N = 336$ K.

DOI: 10.1103/PhysRevB.85.134518 PACS number(s): 75.10.Pq, 74.72.Cj, 75.25.−j, 75.47.Lx

I. INTRODUCTION

Lamellar copper oxides have been extensively studied not only regarding high-critical-temperature (T_c) superconductivity, but also regarding low-dimensional quantum magnets. Cupric oxide (CuO) itself exhibits two antiferromagnetic (AF) transitions at Néel temperatures $T_{N1,N2} = 213,230$ K denoting a strong superexchange energy (70 meV) of the Cu-O-Cu coupling.[1] Recently, Kimura *et al*. detected ferroelectricity in CuO for $T_{N1} < T < T_{N2}$ and thus identified CuO as an induced multiferroic.[2] Cu-O is also the key component of high-T_c cuprate superconductors like $YBa_2Cu_3O_x$ (YBCO), $(La,Sr)_2CuO_4$, and $HgBa_2CuO_{4+\delta}$, which are composed of CuO_2 layers. These materials exhibit an antiferromagnetic phase in the underdoped nonsuperconducting regime of the phase diagram, but some groups additionally reported the existence of a commensurate alternate magnetization—probably of orbital nature—in the Cu-O planes of YBCO and $HgBa_2CuO_{4+\delta}$ well in the doping range of superconductivity.[3–6] Another interesting family of lamellar copper oxides are the oxychlorides like $Ba_2Cl_2Cu_3O_4$ and $Sr_2Cl_2Cu_3O_4$ (2234 materials) which are composed of Cu_3O_4 planes interseeded with Ba(Sr) and Cl layers. The magnetic structure of these Cu_3O_4 layers results in two AF ordering temperatures and has been the focus of extensive experimental and theoretical studies (see Refs. 7 and 8 and references therein).

Here we report on the magnetic properties of the alkaline-earth oxocuprate $BaCu_3O_4$, which is composed of Cu_3O_4 layers[9,10] with a different structure than those of the 2234 materials, and, as will be demonstrated, very different magnetic properties. As a matter of fact, $BaCu_3O_4$ exists only as a parasitic phase in YBCO samples,[9] or on thin films grown on top of a suitable, epitaxial perovskite buffer layer.[11] We therefore performed our measurements on YBCO polycrystalline samples and single crystals which were shown to contain $BaCu_3O_4$.

II. METHODS

The magnetization of 13 polycrystalline and six single-crystalline YBCO samples with various oxygen contents (see Table I) was investigated using a 5-T magnetic property measurement system (MPMS) superconducting quantum interference device (SQUID) magnetometer. The polycrystalline samples were prepared at the SPEC-CEA from three different batches of $YBa_2Cu_3O_x$ powder (batches A, B, and C) by compacting the powder into cylinders of 6-mm diameter and 6-mm height and annealing them under appropriate N_2-O_2 mixtures in order to obtain the desired oxygen content. Four different disks of YBCO single crystals (batches D, E, F, and G) with various oxygen contents were obtained from different sources and cut into cubes with an edge length of usually 5 mm. The oxygen content of samples D1, D2, and D3 was changed using a thermobalance.

In the following, the magnetization M will be given in emu/mol and is normalized to the amount of YBCO in moles. Every measurement was started by zero field cooling (ZFC) of the sample. This was followed by a measurement taken during the warming (FW) and cooling (FC) of the sample under the same magnetic field. It should be noted that the magnetic irreversibility of the superconducting wire used for the fabrication of the magnetometer's solenoid produces a small remanent magnetic field in the range of ± 10 Oe. Prior to the measurements at low field, this remanent field was determined by calibration of the magnetometer with a Pd sample, and the field corrected for the remanent field will be referred to as H_{real}.

III. RESULTS

Figure 1 depicts the magnetization of a $x = 6.43$ polycrystalline YBCO sample (C 6.43, see Table I) measured under a magnetic field of 34 Oe as a function of temperature in the range from 300 to 380 K. The FW magnetization M_{FW} after a zero field cooling increases linearly with increasing temperature up to $T \approx 330$ K followed by a second slightly shallower linear increase for $T \geqslant 340$ K. The FC magnetization M_{FC} exhibits a behavior similar to M_{FW} for $T \geqslant 340$ K, but then shows a visible increase of the magnetization at a temperature of $T_t = (337 \pm 1)$ K. In order to investigate this transition quantitatively, we extrapolated the $M(T)$ curve above the transition to 300 K and defined the difference of the FC magnetization at 300 K with respect to this extrapolation as the step height ΔM of the transition. The

TABLE I. Overview of all YBCO samples with T_c being their critical temperature and T_t the temperature of the observed transition (n.d.: transition nondetectable).

Polycrystalline samples			Single crystals		
Name	T_c (K)	T_t (K)	Name	T_c (K)	T_t (K)
C 6.19		340 ± 4	D1 6.35		n.d.
C 6.28		338 ± 2	E 6.5	45 ± 1	335 ± 2
C 6.34		338 ± 1	F 6.6	55 ± 1	n.d.
C 6.43	31 ± 1	337 ± 1	D2 6.6	55 ± 1	334 ± 2
C 6.52	55 ± 1	338 ± 3	D3 6.7	70 ± 1	n.d.
B 6.53	58 ± 1	n.d.	D3 7.0	86 ± 1	n.d.
B 6.56	60 ± 1	n.d.			
A 6.60	61	n.d.			
A 6.68	62 ± 1	n.d.			
A 6.73	68 ± 1	n.d.			
C 6.79	80 ± 1	338 ± 1			
C 6.90	91 ± 1	337 ± 1			
C 7.0	91 ± 1	338.6 ± 1			

step height ΔM of the transition shown in Fig. 1 amounts to $(1.3 \pm 0.1) \times 10^{-3}$ emu/mol.

The inset of Fig. 1 depicts ΔM as a function of the real applied field H_{real} for the same sample, i.e., the remanent magnetic field in the magnetometer's solenoid has been taken into account for these measurements. At first, the step height ΔM increases steeply with increasing magnetic field up to $H_{\text{real}} = \pm 30$ Oe and then saturates at $\Delta M \approx \pm 1$ emu/mol. Since the absolute value of the step height moves within the range of 10^{-6} emu, the transition could not be observed in high field measurements. The temperature of the transition T_t showed no dependence on the magnetic field up to 0.1 T and is given in Table I for each sample.

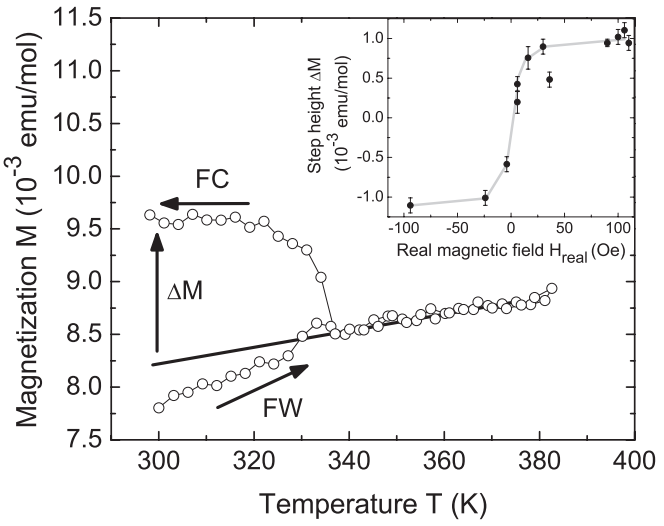

FIG. 1. Field-warmed (FW) and field-cooled (FC) magnetization of the C 6.43 polycrystalline YBCO sample as a function of temperature measured under a magnetic field of $H_{\text{real}} = 34$ Oe after a zero field cooling (ZFC) procedure. Inset: Step height ΔM of the observed transition for the same sample as a function of the real applied magnetic field H_{real} obtained through the same ZFC-FW-FC procedure.

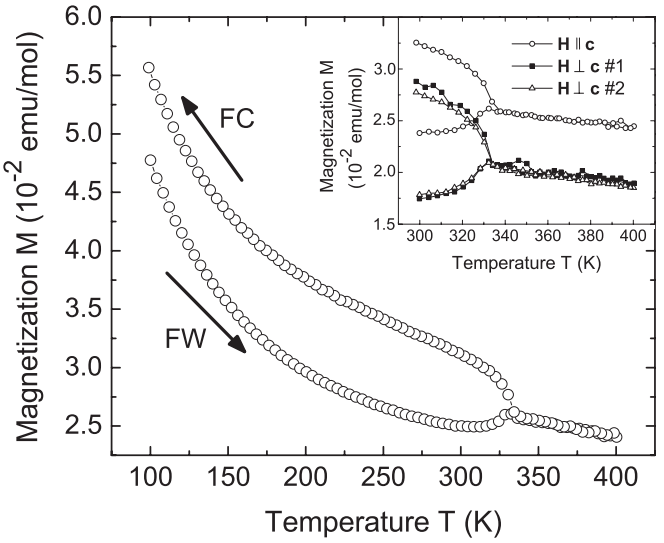

FIG. 2. FW and FC magnetization of the E 6.5 single crystalline YBCO sample as a function of temperature measured under a magnetic field of 50 Oe with $\mathbf{H}\|\mathbf{c}$. Inset: Comparison of the magnetization of the same sample measured under a magnetic field of 50 Oe for $\mathbf{H}\|\mathbf{c}$, $\mathbf{H}\perp\mathbf{c}$ #1, and $\mathbf{H}\perp\mathbf{c}$ #2. The orientations $\mathbf{H}\perp\mathbf{c}$ #1 and $\mathbf{H}\perp\mathbf{c}$ #2 correspond to arbitrary perpendicular directions within the ab plane and not to the **a** and **b** axis of the sample. The initial field cooling was performed here under ≈ -10 Oe resulting in a negative step height in $M_{\text{FW}}(T)$.

Figure 2 shows the magnetization of a $x = 6.5$ YBCO single crystal (E 6.5) as a function of temperature measured under a field of 50 Oe with **H** parallel to the crystals **c** axis. The $M(T)$ behavior is dominated by a strong Curie-Weiss contribution of paramagnetic secondary phases such as the green phase Y_2BaCuO_5 (Ref. 12), $BaCuO_2$ (Ref. 12), and a Curie contribution from free Cu atoms in the Cu chains of YBCO (Ref. 13). In addition, M_{FC} shows a visible transition at a temperature $T_t = (332 \pm 2)$ K. The inset of Fig. 2 depicts the magnetization of the $x = 6.5$ single crystal (E 6.5) measured under a field of 50 Oe for three different orthogonal orientations of the crystal with respect to the magnetic field, clearly revealing the YBCO anisotropy of $M(T)$ between the directions $\mathbf{H}\|\mathbf{c}$ and $\mathbf{H}\perp\mathbf{c}$. However, for all three orientations M_{FC} shows a visible transition at $T_t = (332 \pm 2)$ K with step heights of $\Delta M = (0.6 \pm 0.1) \times 10^{-2}$ emu/mol for $\mathbf{H}\|\mathbf{c}$ and $\mathbf{H}\perp\mathbf{c}$ #2 and $(0.7 \pm 0.1) \times 10^{-2}$ emu/mol for $\mathbf{H}\perp\mathbf{c}$ #1, i.e., there seems to be no visible dependence of the step height on the orientation of the crystal with respect to the magnetic field.

We measured three different batches of polycrystalline YBCO samples and four different batches of single crystals with different oxygen contents x. The transition was only observed for one of the three batches of polycrystalline samples and two of the four batches of single crystals (see Table I), therefore ruling out the origin for the transition as intrinsic to YBCO. Neither the existence nor the temperature of the transition depended on the oxygen content between $x = 0.19$ to $x = 1.0$. (An extensive study about the effects of oxygen disorder on the superconducting and pseudogap properties of YBCO was performed and is described in the companion paper:[14] the present transition temperature was shown to be independent of these effects to within our

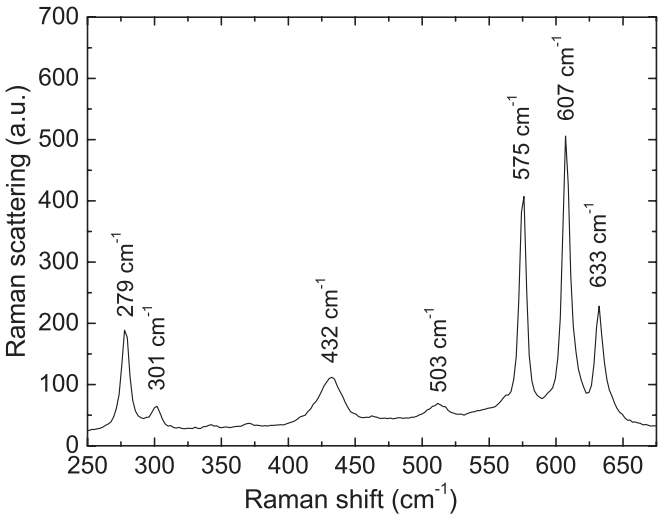

FIG. 3. Raman spectrum of the E 6.5 single crystalline YBCO sample. This spectrum was obtained using a micro-Raman setup and a T64000 triple monochromator. The 514.52-nm line of an Ar-Kr laser was used. The peaks at 279, 503, 575, and 633 cm^{-1} were attributed to $BaCu_3O_4$ (see Ref. 17). The peak at 607 cm^{-1} was attributed to Y_2BaCuO_5 (see Ref. 18), whereas the peaks at 301 and 432 cm^{-1} could not be identified. Similar spectra were obtained only at selected locations on the different samples.

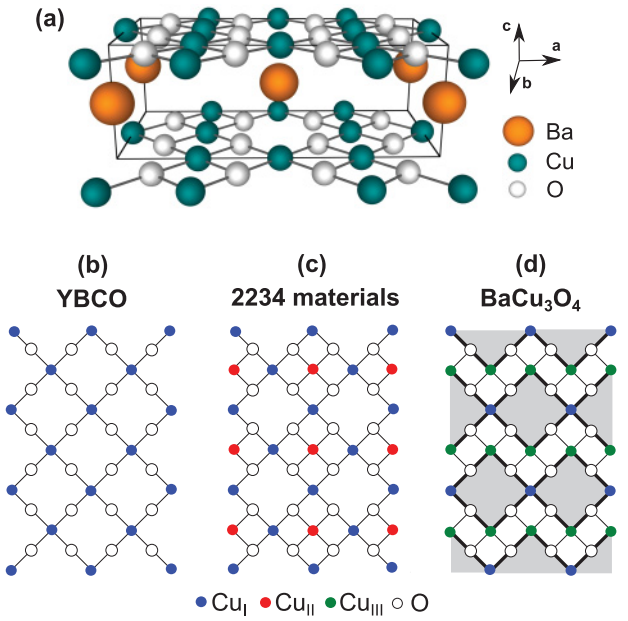

FIG. 4. (Color online) (a) Crystal structure of $BaCu_3O_4$ (Ref. 10). (b) CuO_2 planes in $YBa_2Cu_3O_x$. (c) Cu_3O_4 planes in $Ba_2Cl_2Cu_3O_4$ or $Sr_2Cl_2Cu_3O_4$. (d) Cu_3O_4 planes in $BaCu_3O_4$.

measurement accuracy.) The average temperature T_t of all detected transitions amounts to (336 ± 3) K.

IV. DISCUSSION

Impurity phases present in YBCO have been extensively studied. However, the average temperature of the observed transition of (336 ± 3) K does not match with any of the Néel or Curie temperatures of common impurity phases such as Y_2BaCuO_5 (T_N = 30 K),[12] $Y_2Cu_2O_5$ (T_N = 13 K),[15] $BaCuO_2$ (T_N = 15 K),[16] or CuO ($T_{N1,N2}$ = 213,230 K).[1] This suggests that the transition is either due to an unknown impurity phase or an impurity phase with unknown magnetic properties. As a matter of fact, we detected the presence of the alkaline-earth oxocuprate $BaCu_3O_4$ in samples showing the magnetic transition at (336 ± 3) K using Raman spectroscopy.[17,18] The micro-Raman spectrum is displayed in Fig. 3.

$BaCu_3O_4$ was identified for the first time as a secondary phase in YBCO samples by Bertinotti *et al.* using X-ray diffraction (XRD)[9] and confirmed later.[10] Since $BaCu_3O_4$ is metastable and only grows epitaxially on YBCO or other perovskite structures, there have been only a few studies (among them Raman spectroscopy[17,18]) of this material, and its magnetic properties are unknown. However, as pointed out in Ref. 9, the structure of $BaCu_3O_4$ is close to the structure of the stable materials $Ba_2Cl_2Cu_3O_4$ and $Sr_2Cl_2Cu_3O_4$ (2234 materials) which show a magnetic transition at 330 K[7] and 380 K[8], respectively. $BaCu_3O_4$ consists of Ba and Cu_3O_4 planes [see Fig. 4(a)], whereas the latter are composed of Ba (Sr) planes, Cl planes, and Cu_3O_4 planes. Figure 4 depicts the CuO_2 planes of YBCO [Fig. 4(b)] and the Cu_3O_4 planes of 2234 materials [Fig. 4(c)] and of $BaCu_3O_4$ [Fig. 4(d)]. The CuO_2 layers of YBCO [see Fig. 4(b)] are composed of a square lattice with Cu^{2+} ions (d^9, $S = 1/2$) on the corners (Cu_I sites) and O ions on the edges. Nearest-neighbor (NN) Cu_I ions are coupled via superexchange interaction through the oxygen atom between them, resulting in an AF order below 420 K for YBCO.

Regarding the similarities in the structure of the Cu_3O_4 planes, the magnetic properties of $BaCu_3O_4$ and 2234 materials are expected to bear some resemblances. The Cu_3O_4 planes of 2234 materials [see Fig. 4(c)] consist of the CuO_2 structure shown in Fig. 4(b) with additional Cu ions at the center of every second square (Cu_{II} sites). The Cu_I-O-Cu_I coupling (superexchange energy $J_0 \approx 130$ meV) is similar to that described for the CuO_2 planes of YBCO and results in an AF order below $T_N \approx 330$ and 380 K for $Ba_2Cl_2Cu_3O_4$ (Ref. 7) and $Sr_2Cl_2Cu_3O_4$ (Ref. 8), respectively. The Cu_{II}-Cu_{II} coupling is much weaker ($J_1 \approx 10$ meV) and gives rise to an AF order below $T_N \approx 30$ and 40 K for $Ba_2Cl_2Cu_3O_4$ (Ref. 7) and $Sr_2Cl_2Cu_3O_4$ (Ref. 8), respectively, while no magnetic anomaly is observed in this range of temperature for our samples. Since the interaction of a Cu_{II} ion with the four surrounding Cu_I ions is frustrated, the Cu_I and Cu_{II} sublattices should be decoupled, except for quantum fluctuations.[19] The Cu_3O_4 planes of $BaCu_3O_4$ consist of Cu ions on two different sites, namely, Cu_I and Cu_{III}, and the lattice can be described with "diamond chains" [marked in gray in Fig. 4(d)] consisting of squares attached by their Cu_I corner ions. Cu_I ions are strongly coupled to their four next-NN Cu_{III} ions via a 180° Cu_I-O-Cu_{III} (J_0) superexchange interaction and only weakly coupled to their two NN Cu_{III} ions.

Since the temperature of the observed transition T_t = (336 ± 3) K is close to T_N^I of $Ba_2Cu_3O_4Cl_2$, we attribute T_t to an AF order resulting from the 180° Cu_I-O-Cu_{III} coupling. Unlike the Cu_I and Cu_{II} sublattices in 2234 materials, the Cu_I and

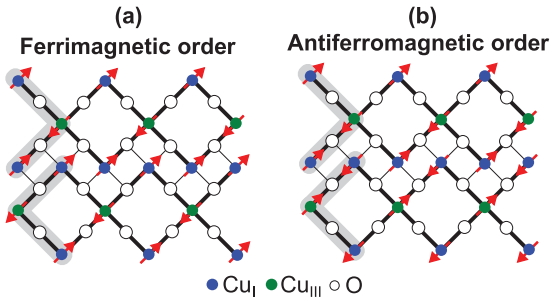

FIG. 5. (Color online) Two possible magnetic orientations of two neighboring diamond chains. Nearest-neighbor chains are (a) ferrimagnetically ordered and (b) antiferromagnetically ordered.

Cu_{III} sublattices in $BaCu_3O_4$ are strongly coupled, resulting in a unique AF order temperature for all Cu ions. Another important difference with respect to the 2234 materials is that in $BaCu_3O_4$ the order is strictly *one dimensional* and not two dimensional. It is noteworthy that the net magnetization of a *single* diamond chain is not zero but one Bohr magneton per three Cu ions, since the cell pattern consists of three Cu ions, one bearing an opposite magnetization with respect to the two others.

There remains the question of the relative ordering of two adjacent and weakly coupled diamond chains. As weak as this interchain coupling may be, it favors the existence of one-dimensional order, which is a key issue inasmuch as such Ising-type order is forbidden when only a pure superexchange mechanism is present (another favoring mechanism may also be the spin-orbit coupling). The first hypothesis for the relative ordering of two adjacent chains is illustrated in Fig. 5(a) and assumes that two NN diamond chains have parallel magnetizations. This would result in a *ferrimagnetic* order and the net magnetization of one Cu_3O_4 layer would be $1/3\ \mu_B$ per Cu. In the case where all layers are similarly oriented, we can estimate the molar fraction of $BaCu_3O_4$ in our samples to be about 2×10^{-6}, which is much too small to be detected by Raman or XRD spectroscopy and therefore not realistic.

The second hypothesis is that the chains have parallel magnetizations within one given layer but the layers are AF ordered. This could in principle give rise to metamagnetism with a "spin-flop" transition at sufficiently high magnetic fields, which was not observed up to 5 T.

The third hypothesis is that the magnetic order of two adjacent chains is antiparallel [see Fig. 5(b)], so that the net in-plane magnetization is zero at zero field and the resulting order within the planes is *antiferromagnetic*. In this case the observed magnetization can be due to the Dzyaloshinskii-Moriya (DM) interaction, which is allowed by symmetry (since the oxygen atom at the center of the Cu_I-O-Cu_{III} bond does *not* bear a center of inversion symmetry) and produces a net out-of-plane moment, able to rotate around the Cu-O bond axis under a magnetic field. This hypothesis of weak ferromagnetism is in fact the only one to be consistent with our observation that the step height ΔM is of the same amplitude for all orientations of the crystal with respect to the magnetic field (see Fig. 2) (note that at zero field the DM contributions of two neighboring chains cancel out). If the third hypothesis is valid, then making the rough assumption that the magnetic step heights ΔM in 2234 materials and in $BaCu_3O_4$ are the same, the molar fraction of $BaCu_3O_4$ in our samples would be about 2×10^{-3}, therefore compatible with Raman observation.

Through neutron scattering measurements on underdoped YBCO, Sidis *et al.*[20] reported coexistence of magnetism and superconductivity at the doping level $x = 6.5$. Part of the sample used for this study is our sample E 6.5 in which we detected $BaCu_3O_4$ through Raman spectrometry (see Fig. 3). The above inferred concentration could also be compatible with the observation of a very small moment through neutron scattering, but too small to be detectable through the muon-spin-resonance (μSR) technique.[20] Since $BaCu_3O_4$ grows epitaxially on YBCO, this also explains the commensurability of the reported magnetic order. This newly discovered magnetic transition in $BaCu_3O_4$ might then account for some cases of apparent coexistence of magnetism and superconductivity in underdoped YBCO.

From the theoretical point of view, according to the pioneering work of Takano and coworkers[21] on the phase diagram of diamond chains, $BaCu_3O_4$ appears indeed to belong to the ferrimagnetic case; however, chain interactions deserve further study.

V. CONCLUSION

We reported on the magnetic properties of $BaCu_3O_4$, a common parasitic phase in $YBa_2Cu_3O_x$ samples. The magnetic order that sets in at 336 K is most probably due to diamond chains of antiferromagnetically coupled Cu 1/2 spins. The measured magnetization may be attributed to either ferrimagnetic ordering or (most probably) antiferromagnetic ordering of adjacent chains in the presence of the Dzyaloshinsky-Moriya interaction yielding weak ferromagnetism behavior. These diamond chains represent a new remarkable system of weakly coupled one-dimensional magnetic objects where AF ordering of the Cu^{2+} ions in each diamond chain leads to a net magnetic moment of each chain.

ACKNOWLEDGMENTS

This work was supported through a SESAME grant from Region Ile-de-France. We gratefully thank P. Bourges, Y. Gallais, A. Sacuto, X. Chaud, and F. Mila for stimulating discussions or experimental collaboration.

*brigitte.leridon@espci.fr

[1] B. X. Yang, T. R. Thurston, J. M. Tranquada, and G. Shirane, Phys. Rev. B **39**, 4343 (1989).

[2] T. Kimura, Y. Sekio, H. Nakamura, T. Siegrist, and A. P. Ramirez, Nat. Mater. **7**, 291 (2008).

[3] B. Fauqué, Y. Sidis, V. Hinkov, S. Pailhes, C. T. Lin, X. Chaud, and P. Bourges, Phys. Rev. Lett. **96**, 197001 (2006).

[4] H. A. Mook, Y. Sidis, B. Fauqué, V. Baledent, and P. Bourges, Phys. Rev. B **78**, 020506 (2008).

[5]Y. Li, V. Balédent, N. Barisic, Y. Cho, B. Fauqué, Y. Sidis, G. Yu, X. Zhao, P. Bourges, and M. Greven, Nature **455**, 372 (2008).
[6]Y. Li *et al*., Nature **468**, 283 (2010).
[7]T. Ito, H. Yamaguchi, and K. Oka, Phys. Rev. B **55**, R684 (1997).
[8]F. C. Chou *et al*., Phys. Rev. Lett. **78**, 535 (1997).
[9]A. Bertinotti, J. Hammann, D. Luzet, and E. Vincent, Physica C **160**, 227 (1989).
[10]F. Yakhou, V. Plakhty, A. Stratilatov, P. Burlet, J. P. Lauriat, E. Elkaim, J. Y. Henry, M. Vlasov, and S. Moshkin, Physica C **261**, 315 (1996).
[11]S. V. Samoylenkov, O. Yu. Gorbenko, I. E. Graboy, A. R. Kaul, H. W. Zandbergen, and E. Connolly, Chem. Mater. **11**, 2417 (1999).
[12]S. S. P. Parkin, E. M. Engler, V. Y. Lee, and R. B. Beyers, Phys. Rev. B **37**, 131 (1988).
[13]B. Leridon, P. Monod, D. Colson, and A. Forget, Europhys. Lett. **87**, 17011 (2009).
[14]J. Biscaras, B. Leridon, D. Colson, A. Forget, and P. Monod, Phys. Rev. B **85**, 134517 (2012).
[15]R. Troć, Z. Bukowski, R. Horyń, and J. Klamut, Phys. Lett. A **125**, 222 (1987).
[16]Z. R. Wang, D. C. Johnston, L. L. Miller, and D. Vaknin, Phys. Rev. B **52**, 7384 (1995).
[17]B. Güttler, S. V. Samoylenkov, and O. Yu. Gorbenko, Physica C **324**, 123 (1999).
[18]H. Rosen, E. M. Engler, T. C. Strand, V. Y. Lee, and D. Bethune, Phys. Rev. B **36**, 726 (1987).
[19]E. F. Shender, Zh. Eksp. Teor. Fiz. **83**, 326 (1982) [Sov. Phys. JETP **56**, 178 (1982)].
[20]Y. Sidis, C. Ulrich, P. Bourges, C. Bernhard, C. Niedermayer, L. P. Regnault, N. H. Andersen, and B. Keimer, Phys. Rev. Lett. **86**, 4100 (2001).
[21]K. Takano, K. Kubo, and H. Sakamoto, J. Phys. Condens. Matter **8**, 6405 (1996).